reduced pressure gave 0.52 g (54%) of the desired acid as an oily mixture containing the *E* and *Z* isomers in a 55:45 ratio: ^{1}H NMR ($CDCl_3$) δ 1.52 (m, 2 H), 1.66 (m, 2 H), 2.39 (m, 4 H), 5.35 (m, 1 H), 6.47 (d of t, J = 7.6, 10.8 Hz, 0.45 H), 6.70 (d of t, J = 6.9, 16.5 Hz, 0.55 H); high-resolution MS calcd for $(M + 1)^+$ peak of $C_8H_{11}NO_2$ 154.0869, found 154.0870.[25]

1-[[(6-Cyano-5-hexenyl)carbonyl]oxy]-2(1*H*)-pyridinethione (8) was prepared by the standard method[2b] by reaction of the above acid with *N*-hydroxypyridine-2-thione and dicyclohexyl carbodiimide with catalytic (10 mol %) DMAP in benzene. The oily product was isolated as a 55:45 (*E*:*Z*) mixture of isomers by silica gel chromatography (1:1 ethyl acetate-hexanes elution) in 55% yield: ^{1}H NMR ($CDCl_3$) δ 1.60 (m, 2 H), 1.78 (m, 2 H), 2.28 (d of d, J = 5, 10 Hz, 1 H), 2.46 (d of d, J = 5, 10 Hz, 1 H), 2.71 (d of d, J = 4, 9 Hz, 2 H), 5.37 (m, 1 H), 6.48 (d of t, J = 7.3, 10.7 Hz, 0.45 H), 6.61 (m, 1 H), 6.70 (d of t, J = 6.9, 16.4 Hz, 0.55 H), 7.23 (m, 1 H), 7.55 (t, J = 5.7 Hz, 1 H), 7.64 (d, J = 7.9 Hz, 1 H).

2-Heptenenitrile (10) was prepared as previously reported.[19] The crude product was purified by column chromatography on silica gel (pentane elution). GC and ^{1}H NMR analyses showed a 60:40 (*E*:*Z*) ratio of isomers; the *Z* isomer eluted before the *E* isomer on a Carbowax GC column: ^{1}H NMR ($CDCl_3$) δ 0.87 (m, 3 H), 1.35 (m, 4 H), 2.15 (m, 1 H), 2.22 (m, 1 H), 5.27 (m, 1 H), 6.43 (d of t, J = 7.7, 10.8 Hz, 0.40 H), 6.66 (d of t, J = 6.9, 16.2 Hz, 0.60 H); MS of *Z* isomer, *m/e* (rel intensity) 109 (1, M^+), 108 (6), 94 (12), 80 (10), 69 (17), 68 (20), 67 (100), 56 (88); MS of *E* isomer, *m/e* (rel intensity) 109 (2, M^+), 108 (4), 94 (8), 80 (8), 69 (17), 68 (18), 67 (49), 56 (100).

Cyclopentylacetonitrile (11) was prepared as previously described.[19] The crude product was purified by chromatography on alumina (1:3, ethyl-pentane solution). ^{1}H NMR ($CDCl_3$) δ 1.31 (m, 2 H), 1.65 (m, 4 H), 1.89 (m, 2 H), 2.20 (m, 1 H), 2.39 (d, J = 7.0 Hz, 2 H); MS, *m/e* (rel intensity); 109 (1, M^+), 108 (15), 94 (9), 80 (13), 69 (100).

Kinetic Studies followed the general procedures previously reported[2b,21] with the exception that the trapping agents were added as stock solutions in the appropriate solvent that were prepared immediately before use. Following visible-light irradiation, the reaction tubes were cooled to -78 °C and opened immediately before GC analysis. Reactions of PTOC **1** were analyzed on the $AgNO_3$ columns; products were identified by the known GC retention times.[2b] Reactions of PTOC **8** were analyzed on the Carbowax column for quantification; products were identified by GC coinjection with authentic samples and by GC-mass spectrometry. Yields were determined relative to an internal standard of benzene or nonane (for PTOC **1** reactions) or dodecane (for PTOC **8** reactions). The GC response factors for **6** and **7** were assumed to be equal to one another and to the standard. The GC response factors for **10** and **11** were determined with authentic samples.

Acknowledgment. We thank the National Science Foundation (CHE-8816365 and CHE-9117929) for support. Xu Yue was a Robert A. Welch Undergraduate Scholar.

Spectroscopic Determination of Solute-Fluid Cluster Size in Supercritical N_2O

Thomas A. Betts, JoAnn Zagrobelny, and Frank V. Bright*

Contribution from the Department of Chemistry, Acheson Hall, State University of New York at Buffalo, Buffalo, New York 14214. *Received April 9, 1992*

Abstract: In supercritical fluids, near the critical point, there exists a region where the interactions between a solute and the surrounding solvent are such that the solvent molecules collapse about the solute. This enhancement of local solvent density, or solvent clustering, is an intriguing phenomena and may prove useful in separations, extractions, and reaction processes. We present here a means to experimentally determine the size of a solute-solvent cluster in the near-critical region using relatively straightforward spectroscopic techniques. In this work the solute, 6-propionyl-2-(dimethylamine)naphthalene (PRODAN), is fluorescent. Therefore, we can use fluorescence anisotropy and lifetime measurements to determine the rotational correlation time of PRODAN in supercritical N_2O. The recovered rotational correlation time is in turn related to the volume of the rotating species if the viscosity of the medium is known. Two limiting cases describing the observed rotational diffusion are considered. In the first, we assume a situation with minimal interaction between the solute and solvent. Second, we investigate the case where the solute and solvent interact strongly. Analysis of the experimental data within this framework allows us to determine the lower and upper volume limits of a solvent cluster. By using the sensitivity of the PRODAN emission spectrum, to the local solvent environment, we determine the density directly surrounding the solute (i.e., the local density). In the region near the critical point, the local density of N_2O about PRODAN is enhanced approximately 2.5-fold compared to the bulk. From the experimental local solvent density and cluster volumes, one has a means to calculate the average number of excess solvent molecules making up a cluster. Based on the two limiting cases, average cluster sizes between 25 and 103 N_2O molecules occur near the critical pressure, and decrease with increasing pressure.

Introduction

Supercritical fluids have properties which are intermediate of gases and liquids.[1-3] Gas-like viscosity and diffusivity coupled with liquid-like solvation power yield a medium that is an appealing alternative to conventional solvents used in chromatography[1-6] and industrial extraction processes.[7-9] Applications in these areas have blossomed over the past decade, preceding a detailed understanding of the underlying solvation processes (i.e., solute-solvent interactions).

The discovery of an interesting phenomenon[10,11] which occurs very near the critical temperature (T_c) and pressure (P_c) has sparked much interest in understanding the molecular-level interactions between solutes and supercritical fluids. In this work, Eckert and co-workers[10,11] found that, at infinite dilution, the partial molar volume of the solute (naphthalene, camphor, or

* Author to whom all correspondence should be directed.

(1) Gouw, T. H.; Jentoft, R. E. *J. Chromatogr.* **1972**, *68*, 303-323.
(2) Klesper, E. *Angew. Chem., Int. Ed. Engl.* **1978**, *17*, 738-746.
(3) van Wassen, U.; Swaid, I.; Schneider, G. M. *Angew. Chem., Int. Ed. Engl.* **1980**, *19*, 575-658.
(4) Peadon, P. A.; Lee, M. L. *J. Liquid Chromatogr.* **1982**, *5*, 179-221.
(5) Novotny, M.; Springston, S. R.; Peadon, P. A.; Fjeldsted, J. C.; Lee, M. L. *Anal. Chem.* **1981**, *53*, 407A-414A.
(6) Fjeldsted, J. C.; Lee, M. L. *Anal. Chem.* **1984**, *56*, 619A-628A.
(7) Eckert, C. A.; Van Alsten, J. G.; Stoicos, T. *Environ. Sci. Technol.* **1986**, *20*, 319-325.
(8) McHugh, M. A.; Krukonis, V. J. *Supercritical Fluid Extraction: Principles and Practice*; Butterworths: Stoneham, MA, 1986.
(9) Williams, D. F. *Chem. Eng. Sci.* **1981**, *36*, 1769-1788.
(10) Eckert, C. A.; Ziger, D. H.; Johnston, K. P.; Ellison, T. K. *Fluid Ph. Equil.* **1983**, *14*, 167-175.

0002-7863/92/1514-8163$03.00/0

tetrabromomethane dissolved in supercritical CO_2 and C_2H_4 at infinite dilution) becomes very large and negative near the critical point. Others have reported similar observations for a host of solutes in a variety of supercritical fluids.[12-16] The existence of large negative partial molar volumes was interpreted in terms of the fluid colapsing and clustering about the solute. However, partial molar volume is a macroscopic property and tells little about the system at the microscopic level. In spite of this, Eckert et al.[10,11] were able to use partial molar volume data to estimate that these solute–fluid clusters are made up of about 100 fluid molecules.

More recently, Debenedetti[17] used fluctuation theory to derive a relationship between solute partial molar volume and cluster size. Again, the experimental partial molar volumes for naphthalene and tetrabromomethane[11] in CO_2 were used and yielded a maximum cluster of 110 fluid molecules. Cluster size, in this respect, describes the number of fluid molecules in the cybotactic region (the region of solvent where structure is influenced by the solute) *in excess* of the solvent ordinarily present based on the bulk solvent density. These cluster sizes are in close agreement with the earlier estimation by Eckert et al.;[10] however, each method was based upon the macroscopic property, partial molar volume.

In this paper, the term "clustering" refers to the situation in which the composition or concentration of the fluid is enriched, relative to the bulk, in close proximity to the solute. However, it is important that one realize that these so-called clusters are dynamical. That is, they are not rigid entities with a well-defined structure; fluid exchange occurs between the cluster and bulk fluid on a picosecond time scale.[18]

Spectroscopic methods provide a convenient means to probe solute–fluid interactions at the molecular level. Thus, optical spectroscopy has been used to study solute–solvent clustering and characterize the cybotactic region in pure[19-36] and cosolvent-modified[37-42] supercritical fluids. For example, Kim and Johnston[19] used the solvatochromic nature of phenol blue to study solute–solvent interactions in supercritical C_2H_4, $CClF_3$, and CF_3H. The local solvent density about this probe was estimated from the phenol blue absorbance spectrum in the supercritical fluid by comparison to theoretical calculations based on the McRae–Bayliss solvent continuum model.[43] This model describes the solvent as a homogeneous polarizable dielectric. From this comparison it was evident that, at reduced pressures ($P_r = P/P_c$) close to unity, the density directly surrounding the solute was significantly greater than the bulk.[19] As solvent pressure was increased, the local density eventually approached that of the bulk. This enhanced local solvent density surrounding the solute is a direct manifestation of the collapse of solvent molecules about the solute (clustering). The solvatochromic absorbance properties of several other solute molecules, 4-(dimethylamino)benzonitrile (DMABN)[20] and 2-nitroanisole,[21-23] have also been used to estimate local solvent density and characterize the solvent strengths of a wide variety of supercritical fluids.

Fluorescence spectroscopy has been used to study solute–solvent interactions in supercritical fluids. As examples, the fluorescence from the twisted-intramolecular charge-transfer state of DMABN[24,25] was used to probe the solvent structure in the cybotactic region. The shift in the DMABN charge-transfer band was measured in supercritical CF_3H as a function of density. As in the earlier solvatochromic absorbance measurements, the spectral shift was compared to shifts predicted based on a theoretical model assuming a homogeneous dielectric solvent. Analysis indicated that the local solvent density was greater than the bulk near the critical point. The local solvent density approached the bulk solvent density as pressure increased.

The fluorescence characteristics of pyrene have also been used to probe the interactions of supercritical solvents with solute molecules.[26-29] The emission spectrum of pyrene monomer has well-resolved vibrational structure. The 0–0 transition (I_1) is symmetry-forbidden, making it sensitive to the polarity/polarizability of the local solvent environment. Thus, by normalizing the intensity of this solvent-sensitive band to a solvent-insensitive band (I_3), which is allowed by symmetry arguments, one has a means to study directly solute–solvent interactions.[44-48] Brennecke et al.[26,27] used pyrene I_1/I_3 values to investigate solute–solvent interactions in supercritical CO_2, CF_3H, and C_2H_4. Local solvent densities were determined by comparing I_1/I_3 at constant density but two different temperatures. The basic idea is that at a temperature far from the critical temperature, where the compressibility of the solvent is low, I_1/I_3 depends only on bulk solvent properties (e.g., density); there is no clustering. However, at

(11) Eckert, C. A.; Ziger, D. H.; Johnston, K. P.; Kim, S. *J. Phys. Chem.* **1986**, *90*, 2738–2746.
(12) Bensen, S. W.; Copeland, C. S.; Pearson, D. *J. Chem. Phys.* **1953**, *21*, 2208–2212.
(13) Chappelear, D. C.; Elgin, J. C. *J. Chem. Eng. Data* **1961**, *6*, 415–420.
(14) Ehrlich, P.; Fariss, R. H. *J. Phys. Chem.* **1969**, *73*, 1164–1167.
(15) Wu, P. C.; Ehlrich, P. *AIChE J.* **1973**, *19*, 533–540.
(16) Abraham, K. P.; Ehrlich, P. *Macromolecules* **1975**, *8*, 944–946.
(17) Debenedetti, P. *Chem. Eng. Sci.* **1987**, *42*, 2203–2212.
(18) Petsche, I. B.; Debenedetti, P. G. *J. Chem. Phys.* **1989**, *91*, 7075–7084.
(19) Kim, S.; Johnston, K. P. *Ind. Eng. Chem. Res.* **1987**, *26*, 1206–1213.
(20) Kajimoto, O.; Morita, A. *J. Phys. Chem.* **1990**, *94*, 6420–6425.
(21) Yonker, C. R.; Frye, S. L.; Kalkwarf, D. R.; Smith, R. D. *J. Phys. Chem.* **1986**, *90*, 3022–3026.
(22) Smith, R. D.; Frye, S. L.; Yonker, C. R.; Gale, R. W. *J. Phys. Chem.* **1987**, *91*, 3059–3062.
(23) Yonker, C. R.; Smith, R. D. *J. Phys. Chem.* **1988**, *92*, 235–238.
(24) Kajimoto, O.; Futakami, T.; Kobayashi, T.; Yamasaki, K. *J. Phys. Chem.* **1988**, *92*, 1347–1352.
(25) Kajimoto, O.; Yamasaki, K.; Honma, K. *Faraday Discuss. Chem. Soc.* **1988**, *85*, 67–75.
(26) Brennecke, J. F.; Tomasko, D. L.; Peshkin, J.; Eckert, C. A. *Ind. Eng. Chem. Res.* **1990**, *29*, 1682–1690.
(27) Brennecke, J. F.; Eckert, C. A. In *Supercritical Fluid Science and Technology*; Johnston, K. P., Penninger, J. M. L., Eds.; ACS Symposium Series 406; American Chemical Society: Washington, DC, 1989, Chapter 2.
(28) Knutson, B. L.; Tomasko, D. L.; Eckert, C. A.; Debenedetti, P. G.; Chialvo, A. A. In *Supercritical Fluid Technology: Theoretical and Applied Approaches in Analytical Chemistry*; Bright, F. V., McNally, M. E. P., Eds.; ACS Symposium Series 488; American Chemical Society: Washington, DC, 1992, Chapter 5.
(29) Zagrobelny, J.; Bright, F. V. In *Supercritical Fluid Technology: Theoretical and Applied Approaches in Analytical Chemistry*; Bright, F. V., McNally, M. E. P., Eds.; ACS Symposium Series 488; American Chemical Society: Washington, DC, 1992, Chapter 6.
(30) Betts, T. A.; Zagrobelny, J.; Bright, F. V. *J. Supercrit. Fluids* **1992**, *5*, 48–54.
(31) Johnston, K. P.; Kim, S.; Combes, J. In *Supercritical Fluid Science and Technology*; Johnston, K. P., Penninger, J. M. L., Eds.; ACS Symposium Series 406; American Chemical Society: Washington, DC, 1989, Chapter 5.
(32) Okada, T.; Kobayashi, Y.; Yamasa, H.; Mataga, N. *Chem. Phys. Lett.* **1986**, *128*, 583–586.
(33) Hrnjez, B. J.; Yazdi, P. T.; Fox, M. A.; Johnston, K. P. *J. Am. Chem. Soc.* **1989**, *111*, 1915–1916.
(34) Blitz, J. P.; Yonker, C. R.; Smith, R. D. *J. Phys. Chem.* **1989**, *93*, 6661–6665.
(35) Buback, M. *Angew. Chem., Int. Ed. Engl.* **1991**, *30*, 641–653.
(36) Betts, T. A.; Zagrobelny, J.; Bright, F. V. In *Supercritical Fluid Technology: Theoretical and Applied Approaches in Analytical Chemistry*; Bright, F. V., McNally, M. E. P., Eds.; ACS Symposium Series 488; American Chemical Society: Washington, DC, 1992, Chapter 4.
(37) Kim, S.; Johnston, K. P. *AIChE J.* **1987**, *33*, 1603–1611.
(38) Yonker, C. R.; Smith, R. D. *J. Phys. Chem.* **1988**, *92*, 2374–2378.
(39) Tingey, J. M.; Yonker, C. R.; Smith, R. D. *J. Phys. Chem.* **1989**, *93*, 2140–2143.
(40) Levy, J. M.; Ritchey, W. M. *J. High Res. Chromatogr. Chromatogr. Commun.* **1987**, *10*, 493–496.
(41) Betts, T. A.; Bright, F. V. *Appl. Spectrosc.* **1990**, *44*, 1203–1209.
(42) Betts, T. A.; Bright, F. V. In *Supercritical Fluid Technology: Theoretical and Applied Approaches in Analytical Chemistry*; Bright, F. V., McNally, M. E. P., Eds.; ACS Symposium Series 488; American Chemical Society: Washington, DC, 1992, Chapter 8.
(43) McRae, E. G. *J. Phys. Chem.* **1957**, *61*, 562–572.
(44) Nakajima, A. *Bull. Chem. Soc. Jpn.* **1971**, *44*, 3272–3277.
(45) Nakajima, A. *J. Mol. Spectrosc.* **1976**, *61*, 467–469.
(46) Kalyanasundaram, K.; Thomas, J. K. *J. Am. Chem. Soc.* **1977**, *99*, 2039–2044.
(47) Dong, D. C.; Winnik, M. A. *Photochem. Photobiol.* **1982**, *35*, 17–21.
(48) Dong, D. C.; Winnik, M. A. *Can. J. Chem.* **1984**, *62*, 2560–2565.

temperatures close to the critical point, I_1/I_3 is greater for the lower temperature at a given density. Because I_1/I_3 is insensitive to temperature in these solvents,[26,27] the increase is a result of increased solute–solvent interactions due to an increase in the local solvent density.

Recently, Knutson et al.[28] used pyrene emission to quantify the extent of local density augmentation. The experimental local densities recovered in this manner were compared to local densities calculated by molecular dynamics simulations involving the first, second, and third solvation shells. The experimentally recovered density augmentation was consistent with contributions from only the first solvation shell.

Most recently, Betts et al.[30,36] used steady-state *and* time-resolved fluorescence to study solvent clustering in supercritical CF_3H. In this work the solute 6-propionyl-2-(dimethylamine)-naphthalene (PRODAN) is used because its fluorescence properties are extremely sensitive to the local solvent environment.[49] Shifts in the steady-state emission spectra were used to determine the extent of local solvent density enhancement. The fluorescence shifts indicated significant density augmentation (up to 120%) in the highly compressible region near the critical point. The excited-state decay kinetics of PRODAN in supercritical CF_3H was also investigated. Interestingly, the model which best describes the experimental intensity decay is a unimodal continuous distribution. This model is consistent with two possible scenarios. In the first, one has PRODAN molecules experiencing an ensemble of environments with slightly different properties. This could be manifest by a distribution of static (on the time scale of the excited-state lifetime) cluster domains (e.g., sizes). The second secenario involves exchange between, in the simplest case, two different domains on the time scale of the fluorescence lifetime. Here, one has PRODAN interconverting between two different domains (e.g., clustered and bulk) on a time scale similar to the excited-state lifetime.

Based on this previous work, a growing body of evidence supports the idea that supercritical fluids cluster strongly about the solute. That is, in the supercritical region, near the critical temperature and pressure, the local density surrounding a solute can exceed the bulk. In the present investigation, we aim to characterize these solvent clusters. To this end, we report on PRODAN in sub- and supercritical N_2O, using fluorescence anisotropy in concert with time-resolved fluorescence spectroscopy. PRODAN was chosen as our solute because of its extreme sensitivity to its local solvent environment[30,36,49] and its short fluorescence lifetime in N_2O. The fluorescence lifetime of PRODAN in N_2O occurs on the same time scale as PRODAN rotational diffusion, allowing one to conveniently "track" the fast (picoseconds) rotational diffusion in the low viscosity supercritical solvent via fluorescence anisotropy techniques. The solvent, N_2O, was chosen because it is slightly polar, has relatively mild critical conditions, and is a well-known quencher of fluorescence.[50–54] Because of the quenching ability of N_2O, we anticipated that the fluorescence lifetime of PRODAN would fall into a range sufficient to yield a measurable fluorescence anisotropy and in turn rotational correlation time. By investigating this chemical system using fluorescence spectroscopy, we have added to the body of evidence supporting the existence of solute–solvent clusters in supercritical fluids, and have determined experimentally a range of possible cluster sizes in supercritical N_2O. The methodology presented for the determination of cluster size is general and can be used for other systems.

Theory

It has been shown that near the critical point strong interactions of supercritical solvent with solutes lead to solute–solvent clusters.[10–14] These "aggregates" are presumably largest near the critical point where the solute–solvent interactions are strongest,[10–14] and diminish as conditions move away from the critical point. Thus, the size and number of excess solvent molecules are very important physical properties of solvent clustering in supercritical fluids. We present here an approach to characterize the solute–solvent cluster by experimentally determining the volume of the rotating entity.

A relationship between the rotational diffusion of any spherical body and its volume is well established.[55,56] In turn, the volume of the rotor is related to how fast that species can rotationally diffuse in solution:

$$\phi = \eta V/RT \tag{1}$$

In this expression ϕ is the rotational correlation time which is equal to $^1/_6D$ (D is the rotational diffusion coefficient), η is the solvent viscosity, V is the volume of the rotating species, R is the gas constant, and T is the temperature. Thus, by measuring the rotational correlation time, one has a simple means of determining the volume of the species if the temperature and viscosity are known.

One method of determining the rotational correlation time of species which fluoresce is steady-state fluorescence anisotropy.[57,58] The fluorescence anisotropy (r) describes the average angular distance the species rotates during its fluorescence lifetime (τ). From the Perrin equation:[57]

$$r = \frac{r_0}{1 + \tau/\phi} \tag{2}$$

one can determine ϕ, if τ and r_0 are known. The limiting anisotropy, r_0, is the anisotropy measured in the absence of rotational diffusion, and describes the angle between the absorption and emission transition moments. It is a fundamental constant and is measured in a vitrified solvent. Besides r_0, one need only determine r and τ to calculate ϕ. This in turn can be used in eq 1 to yield V.

The actual measurement of steady-state fluorescence anisotropy involves excitation of the sample with polarized light. The parallel ($I_\parallel$) and perpendicular ($I_\perp$) components of the fluorescence are then used to determine r:[58]

$$r = \frac{I_\parallel - I_\perp}{I_\parallel + 2I_\perp} \tag{3}$$

In essence, r is a measure of the depolarization of the fluorescence resulting from rotational diffusion (Brownian motion). The larger the emitting species, the slower it will rotationally diffuse, and the less depolarized the emission (bigger r). Thus, because the anisotropy can be directly related to the volume of the rotating entity by eqs 1 and 2, it is a potentially useful tool to study solute–solvent clustering in supercritical fluids. In effect, if the average volume of the cluster were to change, it should be possible to monitor and quantify that change directly if one measures r, τ, r_0, η, and T.

From the Perrin expression (eq 2), it is evident that one must measure r and τ in order to determine ϕ. In this study, τ is measured using the frequency-domain technique.[59–63] To recover

(49) Weber, G.; Farris, F. J. *Biochemistry* **1979**, *18*, 3075–3078.
(50) Husain, D.; Roberts, G. *Chem. Phys.* **1989**, *138*, 187–202.
(51) Menghini, M.; Montone, A.; Morales, P.; Nencini, L.; Dore, P. *Chem. Phys. Lett.* **1988**, *150*, 204–210.
(52) Sester, D. W.; Lin, D. *J. Phys. Chem.* **1985**, *89*, 1561–1564.
(53) Sester, D. W.; Cha, H. *J. Phys. Chem.* **1989**, *93*, 235–244.
(54) Freitag, F.; Rohrer, F.; Stuhl, F. *J. Phys. Chem.* **1989**, *93*, 3170–3174.
(55) Einstein, A. *Ann. Phys.* **1906**, *19*, 371.
(56) Debye, P. *Polar Molecules*; Chemical Catalog Co.: New York, 1929; p 84.
(57) Perrin, F. *J. Phys. Radium* **1926**, *7*, 390.
(58) Lakowicz, J. R. *Principles of Fluorescence Spectroscopy*; Plenum Press: New York, 1983; p 112.
(59) Bright, F. V.; Betts, T. A.; Litwiler, K. S. *C.R.C. Crit. Rev. Anal. Chem.* **1990**, *21*, 389–405.
(60) Gratton, E.; Jameson, D. M.; Hall, R. D. *Annu. Rev. Biophys. Bioeng.* **1984**, *13*, 105–124.
(61) Jameson, D. M.; Gratton, E.; Hall, R. D. *Appl. Spectrosc. Rev.* **1984**, *20*, 55–106.
(62) Federson, B. A.; Piston, D. W.; Gratton, E. *Rev. Sci. Instrum.* **1989**, *60*, 2929–2936.

τ, the experimental phase and modulation data are fit to an assumed decay model using a commercially available nonlinear least-squares fitting algorithm (Globals Unlimited, Urbana, IL). In this approach, the experimental phase angles and demodulation factors are compared to theoretical phase angles and demodulation factors by means of the reduced chi-squared (χ_r^2) function.[59-61,64] The fit producing the lowest χ_r^2 with the fewest number of fitting parameters is traditionally accepted as the best fit.[59-61,64]

Many fluorescent solutes can be used to probe the average local solvent environment by following shifts in their spectra.[24-30,49,65-70] The difference in energy between absorbance and emission (Stokes' shift) is influenced by interactions between the solvent and the solute. Factors affecting this energy difference include (1) general solvent effects which are always present (e.g., vibrational relaxation, redistribution of solvent electrons, and reorientation of solvent dipoles) and (2) specific solvent effects which depend on the chemical structure of the solute and solvent (e.g., hydrogen bonding and energy transfer). The system investigated in this work was chosen in part because specific solvent effects are minimal. Therefore, a brief description of general solvent effects on the Stokes' shift is presented.

The most widely used treatment describing the effect that solvent exerts on the Stokes' shift is from Lippert:[71]

$$\nu_a - \nu_f = \frac{2}{\hbar c}\left[\frac{\epsilon - 1}{2\epsilon + 1} - \frac{n^2 - 1}{2n^2 + 1}\right]\frac{(\mu^* - \mu)}{a^3} + \text{constant} \qquad (4)$$

In this expression, $\nu_a - \nu_f$ is the Stokes' shift (in cm^{-1}), $\hbar$ is Planck's constant, c is the speed of light, ϵ is the solvent dielectric constant, n is the solvent refractive index, $\mu^* - \mu$ is the difference between the excited- and ground-state dipole moments of the solute, and a is the cavity radius swept out by the solute. The term in brackets is known as the orientation polarizability (Δf):

$$\Delta f = \left[\frac{\epsilon - 1}{2\epsilon + 1} - \frac{n^2 - 1}{2n^2 + 1}\right] \qquad (5)$$

and is linearly related to the Stokes' shift through the Lippert equation. The term involving ϵ accounts for the spectral shift due to reorientation of solvent nuclei and redistribution of solvent electrons, whereas the term involving n accounts for shifts due only to redistribution of solvent electrons. Therefore, Δf describes the spectral shift due to nuclear reorientation of the solvent which dominates the general solvent effects. Hence, the Lippert equation provides an important relationship between physical properties of the local solvent environment (ϵ and n which are themselves strong functions of the solvent density)[24-30,36] and the observed shift in energy (wavelength) between absorbance and emission.

Experimental Section

PRODAN was obtained from Molecular Probes (Eugene, OR), and supercritical fluid chromatography grade N_2O was purchased from Matheson. These reagents were used as received. Acetone, acetonitrile, chloroform, cyclohexane, dimethylformamide (DMF), dimethyl sulfoxide (DMSO), and tetrahydrofuran (THF) were either spectrometric or reagent grade; all were dried over molecular sieve prior to use.

Samples were prepared by pipetting an aliquot of PRODAN dissolved in methanol into a high-pressure optical cell. The optical cell design has been described previously.[72] After complete evaporation of the methanol by heating in an oven to 60 °C overnight, the cell was connected to the remainder of the high-pressure apparatus.[72] Residual oxygen was removed by maintaining a vacuum of 50 μmHg throughout the entire apparatus. The jacketed optical cell was heated to the desired temperature, then filled with N_2O to the desired pressure.

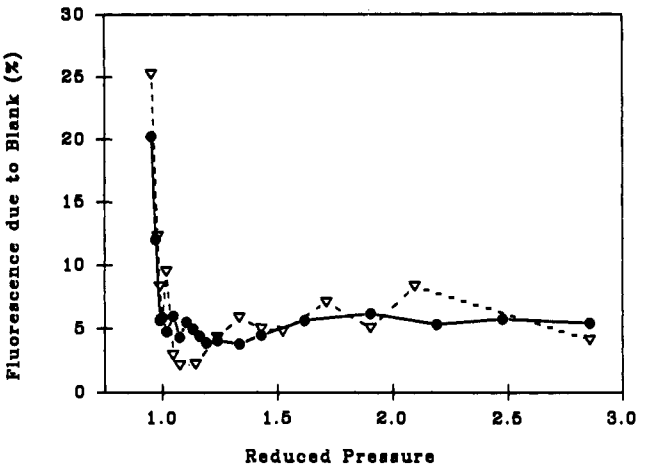

Figure 1. Contribution of background fluorescence from N_2O blank to the total fluorescence intensity: obtained by integrating steady-state emission spectra (●) and from lifetime measurements (▽). λ_{ex} = 351 nm.

All steady-state and dynamic fluorescence measurements were performed on an SLM 48000 MHF spectrofluorometer (SLM Instruments, Urbana, IL) modified to accommodate the high-pressure optical cells.[72] All absorbance measurements were carried out with a Milton Roy 1201 absorbance spectrometer (Milton Roy Co., Rochester, NY).

Three types of fluorescence measurements were needed in these studies: steady-state emission, fluorescence anisotropy, and fluorescence lifetime. In all these measurements a small but relevant contribution to the total fluorescence signal was due to the N_2O blank. The background contribution varied with N_2O pressure; therefore, it was necessary to prepare a blank containing only N_2O under the same experimental conditions as the sample. The sample (with PRODAN) and blank cells were filled simultaneously by means of a plumbing tee placed after the high-pressure pump outlet. All emission spectra in this investigation have been blank subtracted. The emission spectra have further been corrected for the wavelength-dependent response of the emission arm of the fluorometer by means of a standard reference lamp.

Anisotropy measurements were performed in the T-format.[73,74] The T-format was used to compensate for fluctuations in the excitation source. The excitation source was the 351.1-nm line from a CW argon-ion laser (Coherent, Model Innova 90-6). It was necessary to depolarize the laser excitation with a 1-cm thick quartz plate prior to passing the excitation polarizer. A UV band-pass filter was also used to eliminate extraneous plasma discharge. Emission wavelength selection was accomplished with a pair of 385-nm long-pass filters (Oriel) to eliminate any excitation scatter which could potentially bias the anisotropy measurements. Blank subtraction during anisotropy measurements was performed using the software provided with the fluorometer (SLM; version 1.6).

All fluorescence lifetime measurements were performed under magic angle conditions to remove any bias in the observed phase and modulation due to rotational diffusion.[75] Excitation and emission conditions were identical with those used for anisotropy measurements. Phase and modulation data were analyzed using a commercially available nonlinear least-squares software package (Globals Unlimited, Urbana, IL). The goodness-of-fit was judged according to the randomness of the residuals between the measured and calculated phase and modulation as indicated by the reduced chi-squared (χ_r^2).[59-61,64]

Background subtraction is feasible in frequency-domain lifetime measurements;[76] however, it did not prove fruitful in this case owing to the extremely low signal-to-noise in the measurement of the phase angles and demodulation factors of the blank. To circumvent this problem, we measured the phase and modulation in the presence of the background contribution, and modeled the data by a double exponential decay law. One decay component was attributed to PRODAN, and the second was assigned to the N_2O background. Figure 1 compares the fractional contribution of the second lifetime component with the contribution from

(63) Mitchell, G. W. U.S. Patent No. 4,939,457, 1990.
(64) Bevington, P. R. *Data Reduction and Error Analysis for the Physical Sciences*; McGraw-Hill: New York, 1969; pp 187–195.
(65) Bakhshiev, N. G.; Piterskaya, I. V. *Opt. Spectrosc.* **1965**, *19*, 390–395.
(66) Veselova, T. V.; Limareva, L. A.; Cherkasov, A. S.; Shirokov, V. I. *Opt. Spectrosc.* **1965**, *19*, 698–708.
(67) Sun, M.; Song, P. S. *Photochem. Photobiol.* **1977**, *25*, 3–9.
(68) Stryer, L. S. *J. Mol. Biol.* **1965**, *13*, 482–485.
(69) McClure, W. O.; Edelman, G. M. *Biochemistry* **1966**, *5*, 1908–1919.
(70) Brand, L.; Seliskar, C. J.; Turner, D. C. In *Probes of Structure and Function of Macromolecules and Membranes*; Chance, B., Lee, C. P., Blaisie, J. K., Eds.; Academic Press: New York, 1971; pp 17–39.
(71) Lakowicz, J. R. *Principles of Fluorescence Spectroscopy*; Plenum Press: New York, 1983; p 190.
(72) Betts, T. A.; Bright, F. V. *Appl. Spectrosc.* **1990**, *44*, 1196–1202.
(73) Weber, G. *J. Opt. Soc. Am.* **1956**, *46*, 962–970.
(74) Lakowicz, J. R. *Principles of Fluorescence Spectroscopy*; Plenum Press: New York, 1983; pp 128–130.
(75) Spencer, R. D.; Weber, G. *J. Chem. Phys.* **1970**, *52*, 1654–1663.
(76) Swift, K. M.; Mitchell, G. W. Presented at the SPIE Conference, Los Angeles, CA, Jan 1991; paper 1431–19.

Table I. Recovered Fluorescence Anisotropies, Lifetimes, and Rotational Correlation Times for 10 μM PRODAN in N_2O[a]

	T_r = 1.01			T_r = 0.99		
P_r	r	τ (ps)	ϕ^b (ps)	r	τ (ps)	ϕ^b (ps)
0.952	0.024 ± 0.002	505 ± 40	39 ± 6	0.018 ± 0.001	159 ± 14	9.0 ± 1
0.971	0.024 ± 0.002	543 ± 42	42 ± 7	0.018 ± 0.001	149 ± 10	8.4 ± 1
0.990	0.025 ± 0.001	486 ± 39	39 ± 5	0.017 ± 0.001	156 ± 8	8.3 ± 0.9
1.00	0.023 ± 0.002	464 ± 43	34 ± 6	0.017 ± 0.001	153 ± 11	8.2 ± 1
1.01	0.022 ± 0.002	411 ± 102	29 ± 10	0.017 ± 0.001	149 ± 9	7.9 ± 1
1.02	0.022 ± 0.002	358 ± 160	25 ± 13	0.017 ± 0.001	147 ± 6	7.8 ± 0.8
1.05	0.020 ± 0.002	219 ± 19	14 ± 3	0.017 ± 0.001	149 ± 9	7.9 ± 0.7
1.07	0.020 ± 0.002	198 ± 11	13 ± 2	0.017 ± 0.001	154 ± 13	8.2 ± 0.9
1.09	0.019 ± 0.001	169 ± 11	10 ± 1	0.017 ± 0.001	149 ± 12	7.9 ± 1
1.10	0.019 ± 0.001	154 ± 25	9.2 ± 2	0.017 ± 0.001	145 ± 13	7.7 ± 1
1.14	0.019 ± 0.001	183 ± 5	11 ± 0.6	0.018 ± 0.002	170 ± 11	9.6 ± 2
1.19	0.018 ± 0.001	184 ± 1	10 ± 0.7	0.019 ± 0.002	137 ± 10	8.2 ± 1
1.24	0.016 ± 0.002	190 ± 3	9.5 ± 1	0.017 ± 0.001	151 ± 14	8.0 ± 1
1.43	0.016 ± 0.001	209 ± 2	10 ± 0.8	0.017 ± 0.001	137 ± 10	7.2 ± 0.8
1.71	0.015 ± 0.002	191 ± 5	8.9 ± 1	0.017 ± 0.002	142 ± 13	7.6 ± 0.8

[a] All values have been corrected for any measurable N_2O blank. [b] Calculated from eq 2 using r_0 = 0.336 ± 0.002.

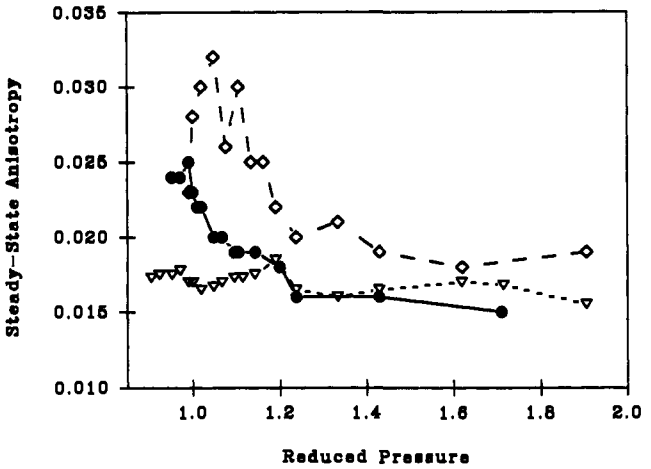

Figure 2. Recovered experimental steady-state fluorescence anisotropy (r) for 10 μM PRODAN in N_2O as a function of reduced pressure at 33.2 (▽), 40.0 (●), and 50.0 (◇) °C. λ_{ex} = 351 nm.

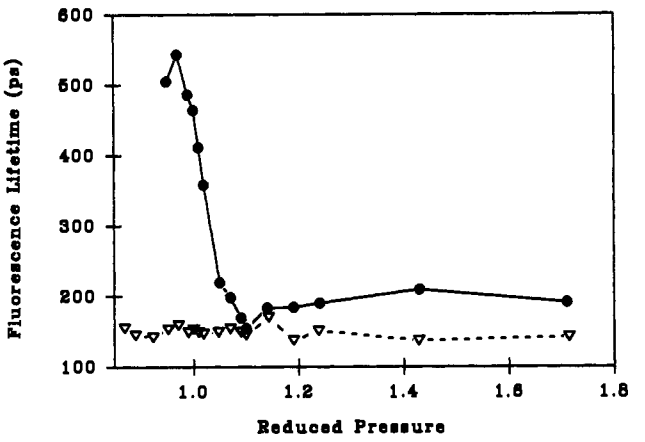

Figure 3. Recovered fluorescence lifetime of 10 μM PRODAN in N_2O as a function of reduced pressure at 33.2 (▽) and 40 (●) °C. λ_{ex} = 351 nm.

the blank as calculated from the sample and blank steady-state emission spectra. The excellent agreement between these two separate measurement schemes supports our assertion that the second recovered lifetime component is due solely to the N_2O background.

Results and Discussion

Before any anisotropy experiments were performed, it was necessary to determine if pressure-induced birefringence of the quartz windows would depolarize the excitation and emission radiation. Pressures in our experiments did not exceed 200 bars; however, others have observed birefringence in quartz at pressures as low as 500 bars.[77-79] We investigated the polarization scrambling of our optical configuration by measuring the anisotropy of a glycogen/H_2O scattering solution in a high-pressure optical cell at atmospheric pressure. The observed anisotropy (0.983) was within instrumental specifications. There was no detectable change in the observed anisotropy as we increased the cell pressure (with N_2) to 200 bars. Temperature-dependent experiments over the same pressure range did not show any evidence of birefringence.

Steady-State Anisotropy. After confirmation of the absence of pressure-induced birefringence in the cell windows, and accounting for the presence of some background fluorescence from the N_2O, the anisotropy of PRODAN in N_2O at temperatures below (33.2 °C) and above (40.0, 50.0 °C) the critical temperature (36.45 °C) were determined as a function of pressure (Figure 2).

The data shown are the average result of three independent sets of experiments and are corrected for all blank contributions. The average anisotropy and associated standard deviations at 33.2 (T_r = 0.99) and 40.0 °C (T_r = 1.01) are also listed in Table I. Two features of these data are worth mentioning. First, the anisotropy of PRODAN in supercritical N_2O decreases with an increase in pressure, whereas in liquid N_2O the anisotropy remains constant. According to eq 2, there are only two possible reasons for a decrease in the observed anisotropy: a decrease in the rotational correlation time (increase in the rate of solute rotational diffusion) or a concomitant increase in the fluorescence lifetime. In order to determine which process underlies the decrease in the observed anisotropy, one must determine the behavior of τ with pressure. The second interesting fact contained in these data is that, in general, r is greater at higher temperatures. Again, this could be due to a decrease in τ or slower rotational diffusion of the solute (increased ϕ). However, in order to draw any solid conclusions from the anisotropy data, the pressure-dependent fluorescence decay times are required.

Fluorescence Lifetimes. The fluorescence decay kinetics of PRODAN in N_2O as a function of pressure were determined at 33.2 and 40.0 °C (Table I). The lifetimes presented in Table I were recovered by fitting the experimental phase angles and demodulation factors to bi-exponential decay models. The bi-exponential decay model offered an average reduction in the χ_r^2 of approximately 40% compared to unimodal Gaussian or Lorentzian lifetime distribution models.[30,36] As stated earlier, one component of the bi-exponential decay law was clearly the contribution from the N_2O background fluorescence (see Figure 1). At each pressure τ was measured twice, and the average τ is presented along with the standard deviation of these independent experiments. Figure 3 graphically compares the fluorescence lifetime of PRODAN

(77) Cantor, D. M.; Schroeder, J.; Jonas, J. *Appl. Spectrosc.* **1975**, *29*, 393-396.
(78) Paladini, A. A.; Weber, G. *Rev. Sci. Instrum.* **1981**, *52*, 419-427.
(79) Eastoe, J.; Robinson, B. H.; Visser, A. J. W. G.; Steytler, D. C. *J. Chem. Soc., Faraday Trans.* **1991**, *87*, 1899-1903.

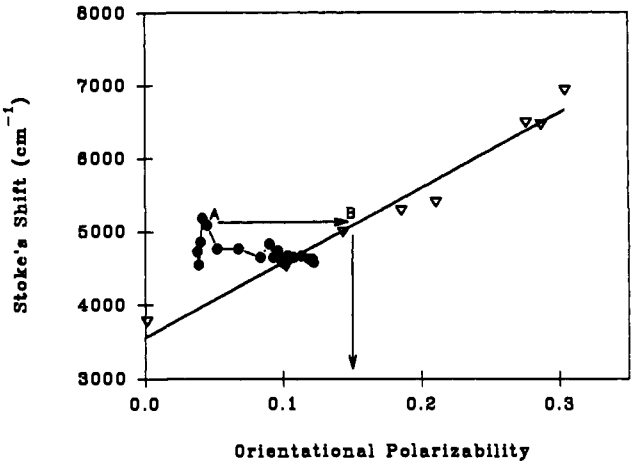

Figure 4. Stokes' shift of 10 μM PRODAN in liquid solvents (▽) (acetone, acetonitrile, chlorobenzene,[48] chloroform, cyclohexane, DMF, DMSO, THF, and triethylamine[48]) and in N_2O as a function of reduced pressure at 40 °C (●).

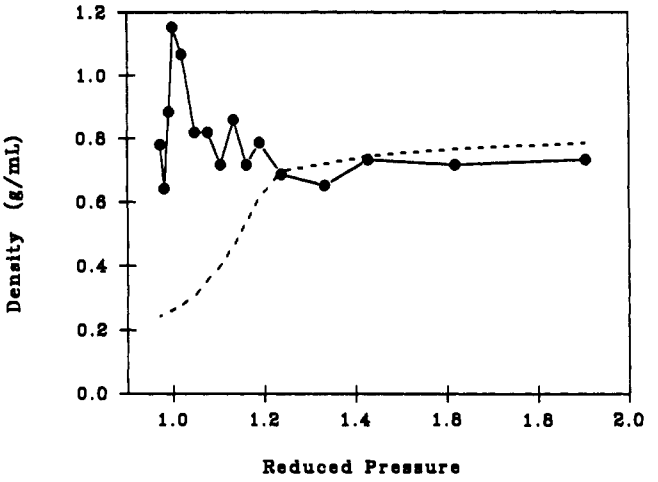

Figure 5. Local N_2O solvent density (●) immediately surrounding PRODAN, and bulk N_2O density[82] (---) as a function of reduced pressure.

in sub- (T_r = 0.99) and supercritical (T_r = 1.01) N_2O as a function of pressure. With our current instrumentation, we were unable to measure τ of PRODAN in N_2O at 50 °C because it is less than our time resolution (≈20 ps). The extremely short τ of PRODAN at elevated temperatures (50.0 °C) is most likely a manifestation of the increased quenching efficiency of N_2O.[50-54]

Additional inspection of these results shows several interesting features. First, in subcritical N_2O (T_r = 0.99, 33.2 °C), τ is short and remains essentially constant with pressure. This indicates that the local environment about PRODAN is not changing appreciable over the pressure range investigated, and is not too surprising considering that N_2O is a liquid under these conditions. Second, for supercritical N_2O (T_r = 1.01, 40.0 °C), as we increase pressure we see a sharp decrease in τ in the vicinity of the critical pressure (P_c = 72.4 bars) (Figure 3). This decrease in τ is a consequence of the dynamical nature of the PRODAN–N_2O quenching phenomena.[50-54] Under these particular conditions, as we increase pressure we simultaneously increase the fluid density and concentration of N_2O, thus leading to a decrease in the excited-state lifetime. However, once we have passed above and away from the critical point, the concentration (density) of N_2O does not increase as rapidly with pressure, and the lifetime levels off at a value near the liquid-phase results.

In previous work from this laboratory,[30,36] we reported that the excited-state decay kinetics for PRODAN in CF_3H was best described by a unimodal distribution of decay times. Thus, one might ask, why do we not observe such a continuous distribution of decay times for PRODAN in N_2O? There are numerous potential reasons (e.g., different polarity of the solvents), but the most likely one is that we simply do not have the time resolution to recover such a distribution in N_2O. Specifically, the average lifetimes for PRODAN in CF_3H and N_2O differ by over an order of magnitude. Thus, if we assume that the relative distribution widths in CF_3H and N_2O are similar, we would require an increase in our upper modulation frequency from the present value of 250 MHz to 2.5 GHz.[59] In effect, we would need to increase our time resolution by about an order of magnitude;[59] this could be accomplished by increasing the upper modulation frequency limit. In short, distinguishing a distribution of decay times from a discrete system on a time scale of a few hundred picoseconds requires enhanced time resolution (1–2 ps) compared to a distributed lifetime centered in the nanosecond regime. Therefore, even if PRODAN in N_2O were to exhibit a distribution of decay times proportional to that seen in CF_3H, it would be beyond the time resolution of our current instrumentation.

Steady-State Absorbance and Emission. In order to estimate local solvent density, the solvatochromic nature of PRODAN is used. This approach is similar to the methodology used to determine local solvent density from solvatochromic absorbance data[31] and follows directly from our work on PRODAN in CF_3H.[36] Here we use the Stokes' shift of PRODAN in a series of aprotic liquid solvents (Figure 4, ▽) of varying orientational polarizability (Δf) as a calibration. According to the Lippert expression (eq 4),[71] these data should be a linear function of Δf. The experimental Stokes' shift for PRODAN in supercritical N_2O has also been determined as a function of density at 40.0 °C (Figure 4, ●). In order to calculate the Δf for N_2O at each density, one needs ϵ and n as a function of density. The dielectric constant was determined from the Debye equation[80,81] as a function of solvent density using the molecular polarizability of N_2O.[82] The corresponding refractive index was calculated from Maxwell's equation[80,81] and the polarizability of N_2O.[82] By comparing the Stokes' shift of PRODAN in supercritical N_2O with that in normal liquids (Figure 4), it is possible to determine the local density of N_2O about PRODAN.

In Figure 4, notice that the Stokes' shift of PRODAN in supercritical N_2O at point A is significantly greater than the shift in a liquid of comparable Δf. That is, the Stokes' shift of PRODAN at point A is comparable to a Δf (and corresponding density) at point B. Thus, the observed Δf for PRODAN in N_2O is greater than the theoretical Δf expected based on the bulk N_2O density. In effect, the local environment about PRODAN is enriched in N_2O and the local density exceeds the bulk. This point is better illustrated in Figure 5 which compares the local N_2O density surrounding PRODAN to that of the bulk.[83,84] For completeness the local N_2O densities about PRODAN as a function of N_2O pressure are compiled in Table II.

These results show clearly that, near the critical point, the local solvent density is significantly greater than the bulk,[85] but approaches the bulk density at higher pressures. The 250% enhancement in local density is slightly higher than previously reported for various solute molecules in other supercritical solvents.[19,24,26,27,30,36] For phenol blue in ethylene, a 60% enhancement in local solvent density was observed;[19] for DMABN in CF_3H,[24] 150%; for pyrene in CO_2,[26,27] 250%; and for PRODAN in CF_3H,[30,36] 120%.

Local Viscosity from Local Density. The enhanced local density will also be manifest in a local viscosity that is increased relative

(80) Atkins, P. W. *Physical Chemistry*; W. H. Freeman: New York, 1986; pp 579–581.
(81) Barrow, G. M. *Physical Chemistry*; McGraw-Hill: New York, 1979; pp 553–555.
(82) Sanyal, N. K.; Dixit, L.; Pandey, A. N. *Ind. J. Pure Appl. Phys.* **1972**, *10*, 329–331.
(83) Couch, E. J.; Kobe, K. A.; Hirth, L. T. *J. Chem. Eng. Data* **1961**, *6*, 229–237.
(84) The average uncertainty in the recovered local density measurements in on the order of ±0.06 g/mL.
(85) The fact that some of the recovered densities exceed 1.0 g/mL should not be any concern because the density of liquid N_2O can exceed 1.2 g/mL: *The Merck Index*; 10th ed., Merck & Co.: Norwood, NJ, 1983.

Table II. Local Density, Viscosity, Cluster Volume, and Size for PRODAN in N_2O at 40 °C

			model 1		model 2	
P_r	ρ_{loc}[a] (g/cm³)	η_{loc}[b] (μP)	V_{loc}[c] (cm³/mol)	N_{loc}[d]	V_{bulk}[e] (cm³/mol)	N_{bulk}[f]
0.952	0.78	696	1430	25	4860	90
0.971	0.78	696	1430	25	5060	94
0.990	0.88	736	1240	24	4560	95
1.00	1.15	883	861	23	3760	103
1.01	1.10	862	735	19	1560	41
1.02	1.07	841	633	16	1360	35
1.05	0.82	715	369	7	960	19
1.07	0.82	715	332	6	640	11
1.09	0.72	657	255	4	440	9
1.10	0.72	591	264	4	509	9
1.14	0.86	720	257	5	390	8
1.19	0.79	697	232	4	300	6
1.24	0.69	566	296	5	290	5
1.43	0.73	607	288	5	310	5
1.71	0.72	599	246	4	210	4

[a] Local density recovered from solvatochromic experiments. [b] Local viscosity recovered from local density. [c] Volume of excess solvent after subtraction of PRODAN volume according to eq 1 using the local viscosity. [d] Number of N_2O molecules involved in cluster from V_{loc}. [e] Volume of excess solvent after subtraction of PRODAN volume according to eq 1 using the bulk viscosity. [f] Number of N_2O molecules involved in cluster from V_{global}.

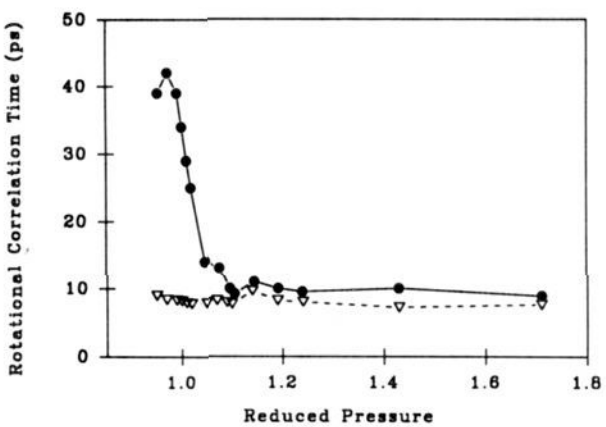

Figure 6. Recovered rotational correlation times for 10 μM PRODAN in N_2O as a function of reduced pressure at 33.2 (▽) and 40 (●) °C.

to the bulk. The pressure–density relationship for N_2O,[83] and the method of Reichenberg[86] were used to calculate the local viscosity corresponding to the recovered local density. Table II collects the results of these calculations. As expected, the viscosity enhancement is greatest in the region nearest the critical point.

Rotational Correlation Times. The experimentally determined r (Figure 2) and τ (Figure 3) of PRODAN in N_2O were used in concert with r_0 to calculate ϕ according to eq 2. The limiting anisotropy for PRODAN dissolved in glycerol at −65 °C (λ_{ex} = 351.1 nm) is 0.336 ± 0.002. The resulting rotational correlation times for PRODAN in sub- (T_r = 0.99) and supercritical (T_r = 1.01) N_2O and associated uncertainties are collected in Table I and illustrated in Figure 6. These results are very interesting and show that the rotational correlation time of PRODAN in subcritical N_2O is absolutely unaffected by pressure. In contrast, the rotational dynamics of PRODAN in supercritical N_2O are strongly dependent on solvent pressure (density). The rotational diffusion is slowest near the critical pressure and decreases as pressure increases.

As stated at the outset, the key goal of this work is to determine the cluster volume. To this end, one must know the temperature and the viscosity of the medium in which the species is rotationally

(86) Reid, R. C.; Prausnitz, J. M.; Poling, B. E. *Properties of Gases and Liquids*; McGraw-Hill: New York, 1987; p 420.

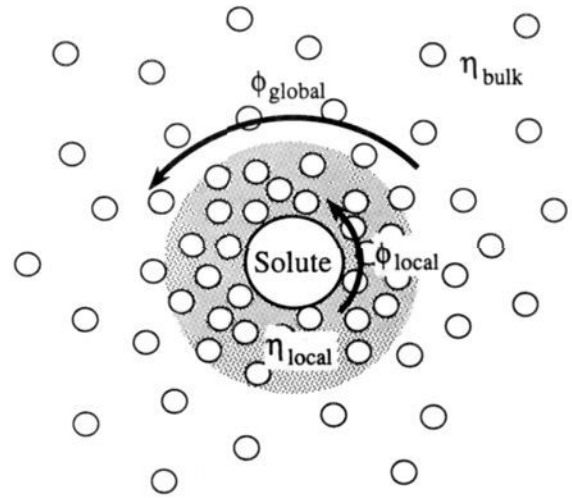

Figure 7. Two models of rotational diffusion of the solute, PRODAN, in a supercritical solvent cluster. ϕ_{local} describes the rotational diffusion of the solute in a medium of local viscosity (η_{local}). ϕ_{global} represents rotational diffusion of the entire solute–solvent cluster in a medium of bulk viscosity (η_{bulk}).

diffusing. The temperature remains constant during a given experiment and can be had straight away; however, the viscosity is not so clearly defined. Specifically, it is not clear what viscosity one may use because the local (in the cybotactic region) viscosity is significantly greater than the bulk in the region near the critical point (vide supra). Thus, we asked, which viscosity (local or bulk) is correct?

To address this issue we investigated two extreme cases of solute–fluid interaction (Figure 7). In the first situation, we assume that there is local motion of the solute in a microscopic region with a local viscosity (η_{local}) greater than the bulk (η_{bulk}). This particular mode of rotational diffusion assumes *minimum* interaction between the solute and the surrounding fluid molecules. The only assumption is that the probe is free to move within the locally enriched environment (cluster). This rotational correlation time is given by ϕ_{local} (Figure 7).

The second case involves *maximum* interaction between the solute and the surrounding solvent cluster. The solute and solvent cluster are considered a single rotating body. According to this global mode of rotational diffusion (given by ϕ_{global}), the bulk viscosity would suffice to calculate the volume of the rotating entity. Thus, although the solute rotational diffusion may be slowed by an increase in the local viscosity, this model assumes the slowing of the rotational diffusion is purely due to an increase in the cluster volume.

Molecular dynamics calculations by Petsche and Debenedetti[18] have shown that supercritical solvent clusters are dynamic in nature. The time scale for a cluster to exchange solvent molecules is on the order of a few picoseconds.[18] That is, the solvent molecules involved in a cluster exchange with the bulk solvent on a picosecond time scale. On the surface, this may seem to contradict the global rotational model described above. However, one must consider the time course of a solvent molecule involved in the cluster. It may participate in the cluster for a few picoseconds, then return to the bulk solvent as another bulk solvent molecule replaces it in the cluster. On average, however, the solvent cluster exists no matter what the identity of the individual solvent molecules. The global rotational diffusion model presented here does not assume that all solvent molecules involved in the cluster remain in the cluster during the rotational diffusion process. A particular solvent molecule may be dragged around with the solute (albeit for only a few picoseconds), before it is replaced by another. The net effect will, of course, be a slowing of the rotational diffusion of the solute due to the summation of the interactions of the individual solvent molecules involved in the cluster with the solute over a long period of time (the average rotational correlation time). Thus, our steady-state fluorescence

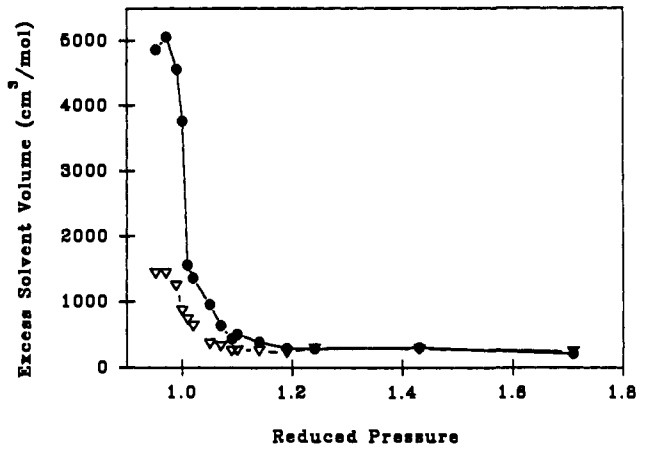

Figure 8. Recovered volume of the excess N_2O solvent clustered about PRODAN as a function of reduced pressure as calculated according to the local (▽) and global (●) models (Figure 7) of rotational diffusion using eq 1.

anisotropy experiments probe only the *average* cluster environment.

The extent to which either the local or global rotational diffusion model contributes to the observed rotational diffusion of the solute is extremely difficult to determine owing to the nature of the present experiments. From our current steady-state anisotropy measurements, we are forced to assume that the decay of anisotropy is described by a isotropic rotor model. One requires superior time resolution and a time-resolved anisotropy experiment to study any picosecond anisotropic rotational diffusion.[87] The steady-state experiments presented in this paper are incapable of making this distinction. However, by studying the two limiting cases (Figure 7) we can easily bracket the minimum and maximum sizes of the supercritical solvent cluster. The actual rotational diffusion of PRODAN in supercritical N_2O probably lies somewhere between the two models of rotational diffusion outlined here.

According to the local rotational diffusion model, the local viscosity and the experimental ϕ were used in eq 1 to determine the volume of the solute–fluid cluster under minimal solute–solvent interaction. Because we are interested in the volume of excess solvent surrounding the solute (the volume of the cluster), the volume of the solute, PRODAN (141 cm³/mol), is subtracted from the total volume to give V_{local}. The molecular dimensions of PRODAN were determined through the use of standard bond lengths and angles,[88] van der Waals radii, and basic trigonometry. After subtraction of the solute volume, the volume of the excess solvent V_{local} was calculated (Table II and Figure 8). V_{local} describes the volume of excess solvent rotating with the solute when solute–solvent interactions are *minimal*.

The global rotational diffusion model is treated in a similar manner except the bulk viscosity is used in eq 1 to determine the volume of the rotating species. After subtraction of the solute volume, the volume of excess solvent surrounding the probe, V_{global}, is given in Table II and Figure 8. V_{global} describes the cluster volume when interactions between the solute and solvent are *maximum*. In both cases the solvent cluster volume is maximum near the critical point and decreases with increasing pressure.

From the local density (the density of the cluster) and the solvent cluster volumes (Figure 8), it is possible to determine the average number of solvent molecules participating in the cluster. These results are collected in Table II and presented graphically in Figure 9. Notice that the cluster size determined according to the local rotational diffusion model is significantly smaller

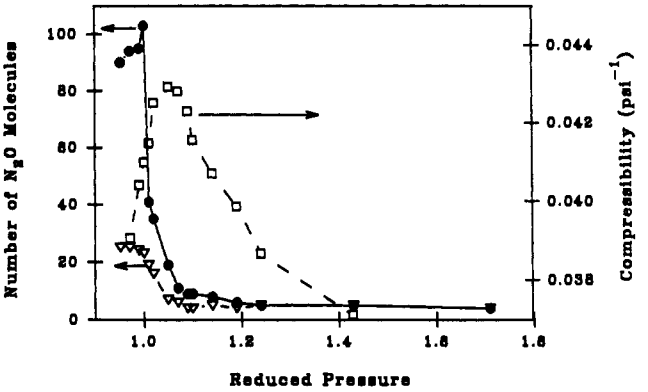

Figure 9. Average number of excess N_2O molecules involved in a cluster about PRODAN as a function of reduced pressure at 40 °C according to local (▽) and global (●) models of rotational diffusion. Isothermal compressibility of N_2O at 40 °C (□).

compared with the global rotational diffusion model. When local motion is assumed, the calculations do not include the solvent volume responsible for the increase in the local solvent viscosity.

Figure 9 also shows the isothermal compressibility[89] of N_2O at 40 °C as a function of reduced pressure. Although the compressibility does not track our experimental cluster size perfectly, it does follow qualitatively; that is, the cluster size decreases rapidly as we move away from the high compressibility region.

Conclusions

In this work we have presented a new method for experimentally determining cluster sizes formed about a solute in a supercritical solvent. Specifically, we report on the fluorescent probe, PRODAN,[90] in supercritical N_2O. By using steady-state fluorescence anisotropies and lifetimes we have provided new evidence for solvent clustering about a solute very near the critical point. From these data and the application of two models of rotational diffusion, a range of possible volumes of the PRODAN-$(N_2O)_x$ cluster was argued. Further, it was shown that, regardless of the rotational diffusion model used, the volume of the solvent cluster is maximum near the critical point, scales as the isothermal compressibility, and decreases with increasing pressure.

Clearly, clustering of fluid molecules about the solute creates a local solvent density in excess of the bulk. The local density has been determined by comparing the Stokes' shifts of PRODAN in supercritical N_2O and a series of aprotic liquid solvents. The local density in the region near the critical point is, on average, 2.5 times the bulk density. However, at elevated pressures, the bulk and local densities do not differ appreciably as the cluster coalesces into the bulk fluid.

From the new solvent cluster volume data and the local density of the fluid about PRODAN, the average number of N_2O molecules involved in the solvent cluster has been determined experimentally. Near the critical point, the cluster involves (depending on the model) between 25 and 103 N_2O molecules, and again, the *average* number of cluster molecules decreases with increasing fluid density.

Interestingly, for naphthalene in supercritical CO_2, Eckert et al.[10] reported a cluster size of approximately 100 solvent molecules. Debenedetti,[17] using fluctuation analysis methods, showed that the cluster size could reach up to 110 solvent molecules based upon Eckert's partial molar volume data.[11] Our results for PRODAN in supercritical N_2O are well within this range. Our upper limit of 103 N_2O molecules, which was calculated according to the global rotational diffusion model, is similar to Eckert and Debenedetti's cluster sizes.[10,11,17] Assuming that CO_2 and N_2O cluster

(87) Subpicosecond fluorescence depolarization experiments based on upconversion techniques have been demonstrated in liquid solvents (cf.; Ruggiero, A. J.; Todd, D. C.; Fleming, G. R. *J. Am. Chem. Soc.* **1990**, *112*, 1003. Hansen, J. E.; Rosenthal, S. J.; Fleming, G. R. *J. Phys. Chem.* **1992**, *96*, 3034.) However, it may prove difficult to dissolve the amounts of solute required for effective upconversion in supercritical solvents.

(88) Pople, J. A.; Beveridge, D. L. *Approximate Molecular Orbital Theory*; McGraw-Hill: New York, 1970; pp 110, 111.

(89) The isothermal compressibility is determined from the density versus pressure/temperature data.[83]

(90) It is possible that the excited-state photophysics for PRODAN follow a twisted intramolecular charge transfer scheme (cf.: Sun, Y.-P.; Fox, M. A.; Johnston, K. P. *J. Am. Chem. Soc.* **1992**, *114*, 1187). If this were the case it would not affect the results for our particular experiments.

similarly, this indicates strongly that the global rotational diffusion dominates our system (ϕ_{global}; Figure 7). That is, the average PRODAN-$(N_2O)_x$ cluster apparently moves as a unit;[91] there is minimal contribution from the PRODAN motion independent of the cluster.

We are currently investigating alternative fluorescent probes for characterization of supercritical CO_2. PRODAN is unacceptable because of its long fluorescence lifetime (≈2 ns) in the interesting region near the critical point. In these experiments, it is imperative that the fluorescence lifetime of the solute probe be on the same time scale as the expected rotational diffusion (tens of picoseconds). If the lifetime is too long, the observed anisotropy will provide no information about rotational diffusion (see eq 2). Thus, we are investigating several short-lived fluorescent probes which emit in the visible, and whose fluorescence lifetime is relatively insensitive to the local environment.

Acknowledgment. Financial support was provided by the U.S. Department of Energy (DE-FGO2-90ER14143) and an Allied Signal Fellowship (T.A.B.). We also acknowledge Bill Fain of SLM Instruments for the calibration lamp.

Registry No. N_2O, 10024-97-2; PRODAN, 70504-01-7.

(91) One should not loose site of the dynamical nature of these clusters.[18] Clearly, there is exchange of fluid species on a picosecond time scale; thus, we can at best only speak about average cluster properties.

The First Direct Observation of Magnetic Field Effects on the Dynamic Behavior of Radical Pairs Involving Group 14 Silicon and Germanium Centered Radicals

Masanobu Wakasa, Yoshio Sakaguchi, and Hisaharu Hayashi*

Contribution from the Molecular Photochemistry Laboratory, The Institute of Physical and Chemical Research (RIKEN), Wako, Saitama 351-01, Japan. *Received April 27, 1992*

Abstract: Laser flash photolysis was performed on micellar solutions and oil emulsions of organosilicon and organogermanium compounds ($(aryl)_nMe_{n-4}E$: E = Si or Ge) in the absence and presence of magnetic fields at room temperature. The dynamic behavior of the silyl and germyl radicals formed upon decomposition of the triplet states was directly observed. The lifetime of the radical pair of group 14 element centered and aryl radicals and the yields of the escaped silyl and germyl radicals were observed to increase with magnetic field strength increasing from 0 to 1.35 T.

Magnetic field effects on the chemical reactions of radical pairs and biradicals have received considerable attention.[1-3] Although extensive studies on the effects have been made previously, there have been only a limited number of studies on the reactions of radicals involving heavy atoms such as Si, S, Ge, and Sn. Recently, we carried out a laser flash photolysis study of phenacyl phenyl sulfone in a micellar solution at room temperature and found magnetic field effects on the yield of the escaped benzenesulfonyl radical.[4] In the reactions involving germyl and ketyl radicals, we also found magnetic field effects on the yield of the ketyl radical.[5] The observed magnetic field effects in these reports, however, were much smaller than those reported in the reactions of ketones in micellar solutions where carbon (C)-centered radicals were produced.[6] It is believed that the deficiencies in the effects are due to the spin-orbit (SO) interaction of heavy atoms such as Si and Ge.[1-3]

The key problem in establishing the importance of magnetic field effects on the reactions involving such heavy atoms is to find a suitable reaction system in which the influence of the SO interaction can be suppressed. Currently, the photochemistry of group 14 element compounds is a very active research area.[7] During the last decade, we have investigated the photochemical reactions of the radicals of heavy atoms such as Si, Ge, and Sn from the viewpoints of intermediates, kinetics, and excited states.[8-17] By means of laser flash photolysis and fluorescence lifetime measurements, we have found that the photolysis of some organosilicon and organogermanium compounds in cyclohexane gives group 14 element centered radicals.[8] In particular, we have found that the photodecomposition of aryl-substituted germanes occurs through the triplet excited states. The primary photochemical processes of these germanes (R_3GeAr)[8] are described in eqs 1-3. Thus, a triplet radical pair of germyl and aryl radicals

$$R_3GeAr \xrightarrow{h\nu} {}^1R_3GeAr^* \rightarrow {}^3R_3GeAr^* \quad (1)$$

$${}^3R_3GeAr^* \rightarrow {}^3\overline{R_3Ge^{\bullet}\cdot Ar} \quad (2)$$

$${}^3\overline{R_3Ge^{\bullet}\cdot Ar} \rightarrow R_3Ge^{\bullet} + Ar^{\bullet} \quad (3)$$

R = aryl or alkyl, Ar = aryl

(1) Steiner, U. E.; Ulrich, T. *Chem. Rev.* **1989**, *89*, 51.
(2) Hayashi, H.; Sakaguchi, Y. *Lasers in polymer science and technology: applications*; CRC Press: Boca Raton, FL, 1990; Vol. 2, Chapter 1.
(3) Hayashi, H. *Photochemistry and photophysics*; CRC Press: Boca Raton, FL, 1990; Vol. 1, Chapter 2.
(4) Hayashi, H.; Sakaguchi, Y.; Tsunooka, M.; Yanagi, H.; Tanaka, M. *Chem. Phys. Lett.* **1987**, *136*, 436.
(5) Hayashi, H.; Sakaguchi, Y.; Mochida, K. *Chem. Lett.* **1984**, 79.
(6) (a) Sakaguchi, Y.; Hayashi, H. *J. Phys. Chem.* **1984**, *88*, 1437. (b) Sakaguchi, Y.; Hayashi, H.; Nagakura, S. *J. Phys. Chem.* **1982**, *86*, 3177.
(7) For example, see: West, R. *Comprehensive Organometallic Chemistry*; Pergamon Press: New York, 1982; Vol. 2, Chapter 9.4.
(8) Mochida, K.; Wakasa, M.; Sakaguchi, Y.; Hayashi, H. *Nippon Kagaku Kaishi* **1987**, *7*, 1171.
(9) Mochida, K.; Wakasa, M.; Sakaguchi, Y.; Hayashi, H. *J. Am. Chem. Soc.* **1987**, *109*, 7942.
(10) Mochida, K.; Wakasa, M.; Nakadaira, Y.; Sakaguchi, Y.; Hayashi, H. *Organometallics* **1988**, *7*, 1869.
(11) Mochida, K.; Yoneda, I.; Wakasa, M. *J. Organomet. Chem.* **1990**, *399*, 53.
(12) Wakasa, M.; Inoue, N.; Mochida, K.; Sakaguchi, Y.; Hayashi, H. *Chem. Phys. Lett.* **1988**, *143*, 230.
(13) Wakasa, M.; Mochida, K.; Sakaguchi, Y.; Nakamura, J.; Hayashi, H. *J. Phys. Chem.* **1991**, *95*, 2241.
(14) Wakasa, M.; Mochida, K.; Sakaguchi, Y.; Hayashi, H. *Bull. Chem. Soc. Jpn.* **1991**, *64*, 1889.
(15) Mochida, K.; Kanno, N.; Kato, R.; Kotani, M.; Yamauchi, S.; Wakasa, M.; Hayashi, H. *J. Organomet. Chem.* **1991**, *415*, 191.
(16) Igarashi, M.; Ueda, T.; Wakasa, M.; Sakaguchi, Y. *J. Organomet. Chem.* **1991**, *421*, 9.
(17) Mochida, K.; Yoshizawa, C.; Tokura, S.; Wakasa, M.; Hayashi, H. *Polyhedron* **1991**, *10*, 2347.

0002-7863/92/1514-8171$03.00/0